

## A Pleistocene origin of the strandflat coastal platform in southwestern Scandinavia

Haakon Fossen<sup>1</sup>✉

An impressively extensive shore platform, the strandflat, is cut 20–50 km into hard crystalline bedrock along most of the Norwegian coastline. Its age and origin have been debated for more than a century, including a model that it represents a weathered, buried and re-exposed Triassic surface. Resolving this issue requires integrated examination of the coastal area together with the offshore Mesozoic rift margin. Here I combine new 3D broadband seismic, bathymetric, and onshore elevation data along coastal West Norway and find that the near-horizontal strandflat postdates both the west-sloping onshore “paleic” surface and the offshore Jurassic denudation surface. It also postdates tilted North Sea Neogene sediments. Consistent with low-temperature thermochronologic data, this shows that the strandflat is a Pleistocene geomorphic feature formed through periods of varying climatic conditions, facilitated by preexisting fault and fracture zones. It is not part of an inherited Mesozoic landscape.

<sup>1</sup>Museum of Natural History, University of Bergen, Allégaten 41, N-5007 Bergen, Norway. ✉email: [haakon.fossen@uib.no](mailto:haakon.fossen@uib.no)

Many coastal landscapes are characterized by a subhorizontal shore platform developed by long-term weathering and wave-dominated erosion, typically of sedimentary or very low-grade metasedimentary rocks. The Norwegian shore platform, the so-called strandflat, developed over a stretch of 1700 km along most of Norway's coast from 59° to 71°N (Fig. 1), is special in the way that it is carved out in hard metamorphic and igneous rocks, that it is not actively forming today (it has preserved fresh Pleistocene glacial striations) and that it is very wide (up to 50 km) and still near horizontal. The strandflat is of fundamental importance for coastal habitation, fishing industry, agriculture, and infrastructure, yet widely different models have been proposed for its age and formation.

Marine abrasion was considered the main process involved by Hans Reusch already in 1894, defining the strandflat as a wave-cut platform of pre-glacial and interglacial origin. Several later researchers<sup>1–5</sup> explained the strandflat as a result of processes related to a cold Quaternary climate, involving erosion by cirque glaciers, frost shattering, and sea-ice. In contrast, others argue that the strandflat represents a Mesozoic landscape feature formed through subaerial denudation and deep weathering, covered by sediments and rejuvenated during later marine or glacial erosion<sup>6–9</sup>. Recently, Fredin et al.<sup>10</sup> obtained K-Ar ages of illite in a narrow fracture zone in a Caledonian granodiorite outcrop in the southernmost portion of the strandflat. They obtained a range of ages from Early Devonian to late Triassic, very similar to K-Ar illite ages from other fracture and fault zones in Western Norway where they have been related to tectonic fault activity<sup>11,12</sup>. Fredin et al.<sup>10</sup> suggested that their youngest illite age date surface weathering in a late Triassic landscape close to the present erosion level, while they consider all older ages as mixed ages (contaminated by host rock mineralogy). This

interpretation is inconsistent with low-temperature geochronologic data from the strandflat area, which suggest that the rocks defining the current strandflat were still deeply buried in the late Triassic<sup>13</sup>. Hence the illite can be explained as a subsurface alteration product related to fluid flow in fault or fracture zones. On the other hand, a thin vertical zone of late Jurassic sediments has been captured in a fault zone near Bergen (Bjørøy)<sup>14</sup>. Hence in places, the structural level currently incised by the strandflat was, by Jurassic time, relatively near the surface of the Earth.

Much of the reason why the Norwegian strandflat and similar shore platforms in other parts of the world are still poorly understood is that previous studies have focused on onshore observations. I believe that the strandflat can only be understood when studied in the context of both onshore and offshore features, and the advent of offshore seismic and bathymetric 3D data is opening new opportunities for such investigations. In this work I consider the full context of the strandflat in Western Norway, i.e., not only its onshore part, but also its submerged shallow-marine part and its offshore relation with the top crystalline denudation surface preserved under Mesozoic sediments of the North Sea rift basin to the west. Our main approach is to digitally integrate and analyze new offshore 3D broadband seismic and stratigraphic data (Supplementary Fig. S1 shows coverage), new nearshore bathymetric data (Supplementary Fig. S2 shows full bathymetry), and onshore elevation data. The new integrated data clearly show that the strandflat in Western Norway is Pleistocene in age with little or no inheritance of Mesozoic landforms.

## Results

The strandflat in Western Norway (Fig. 2a) is a subhorizontal (Fig. 2b) region partly above and partly below the present sea

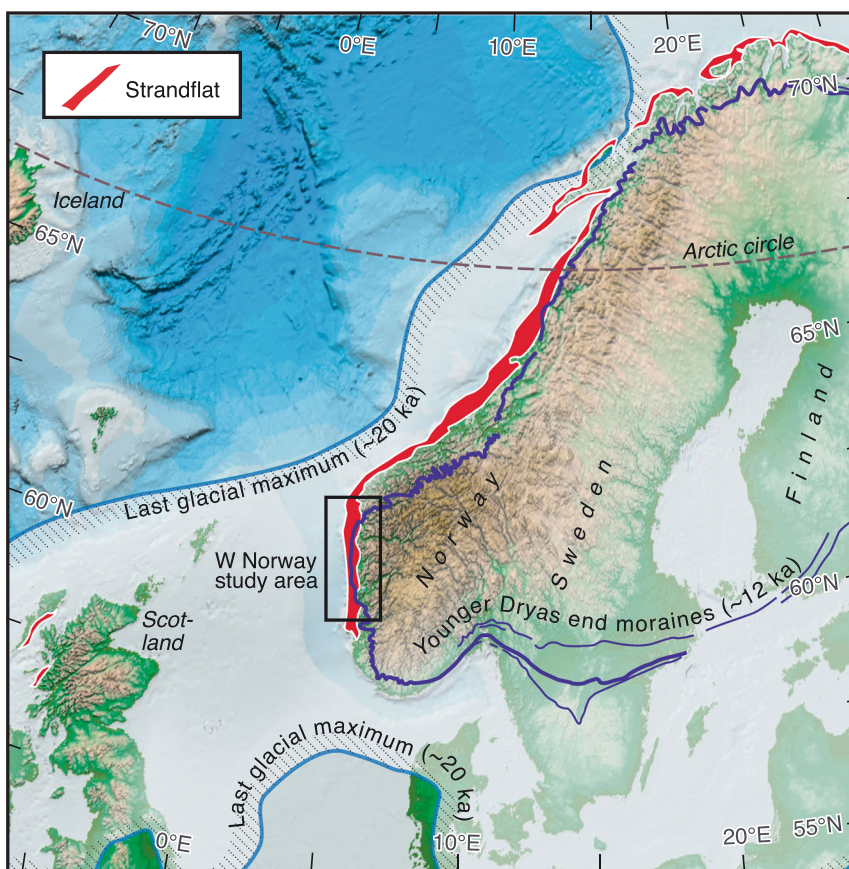


**Fig. 1** Location and extent of the strandflat in western Scandinavia. Occurrence below current sea level is included. Also shown are smaller strandflat sections in Scotland, the last glacial maximum, and Younger Dryas end moraines.

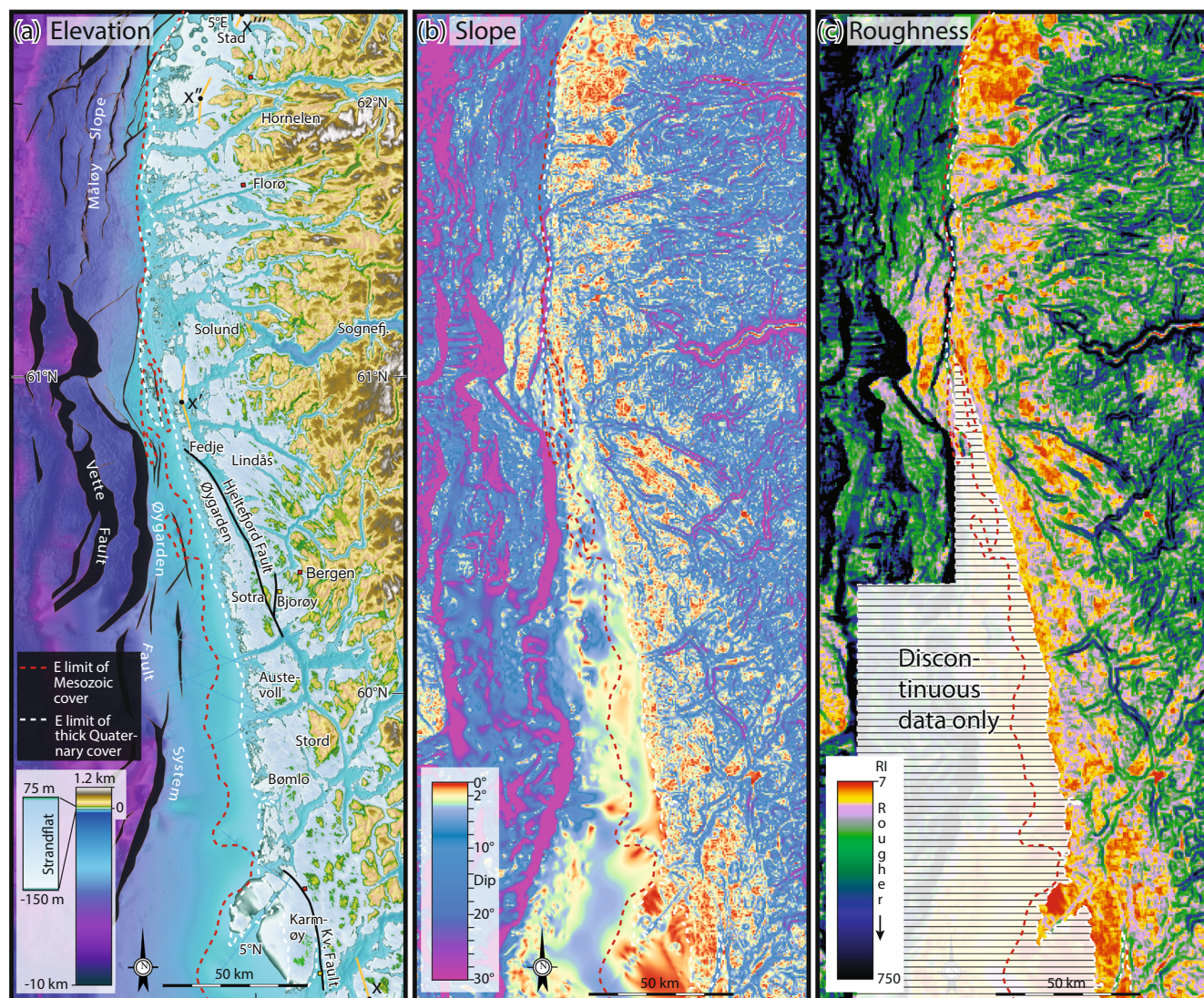


**Fig. 2** Maps of the top crystalline basement in the on-offshore study area. The maps were produced by combining onshore topographic data, nearshore bathymetric data and offshore 3D broadband seismic data. **a** Elevation map of top crystalline basement with the  $-150$  to  $+75$  m interval (containing the strandflat region) marked in light blue. Eastern limits of Mesozoic sediments and of continuous Quaternary cover on basement are shown. **b** Slope (dip) of the landscape, emphasizing the subhorizontal domain (red color) along the coast that closely correlates with the  $-150$  to  $+75$  m elevation interval shown in **a**. **c** Terrain roughness (or ruggedness) index (RI) (Riley et al., 1999), showing a low-relief coastal/near-shore region (warm color) that is markedly less rough than the rest of the region and that to a large extent corresponds with the  $-150$  to  $+75$  m topographic interval shown in (a). Resolution of original elevation data are 10 m onshore and 50 m offshore, resampled to 250 m before calculation of slope and roughness maps to even out small-scale topographic features. Kv. fault; Kvitsøy Fault.

level. It is slightly deeper/lower in the north, where most of it is submerged (Fig. 3). As a whole it ranges from roughly  $-150$  to 60 m elevation, separating two much larger geomorphic provinces: the elevated inland region and the offshore North Sea rift region. Both of these provinces are defined by west-sloping denudation surfaces into which the strandflat has been excavated.

**The Mesozoic offshore denudation surface.** West of the strandflat, a Jurassic denudation surface has been preserved below Mesozoic sediments (Fig. 3). This surface, commonly referred to as top crystalline basement, is the Jurassic topography sculptured on crustal rocks that represent a westward continuation of onshore rocks; Proterozoic to Silurian Paleozoic gneisses, magmatic rocks and schists, and limited amounts of very low-grade

Devonian clastic rocks. This is confirmed through offshore commercial wells drilled to basement. All the cores available from near-shore basement show fresh crystalline rocks with very little sign of weathering (Fig. 4).

The Jurassic unconformity is diachronous, younging towards the mainland, but of early to middle Jurassic age near the coast. It represents a low-relief paleotopographic surface locally affected by erosional channels of Cretaceous age<sup>15</sup>. The unconformity was subjected to late Jurassic to early Cretaceous rift faulting, producing relatively minor east-dipping faults north of Sognefjorden, while major west-dipping faults to the south (e.g., Øygarden Fault) are mainly of early Triassic age with only modest Jurassic-Cretaceous reactivation. The base Jurassic unconformity dips relatively steeply ( $\sim 15^\circ$ ) north of Sognefjorden, as constrained by excellent 3D seismic data that in this area extend close to the coast (Figs. 3 and 5). Most of the strong

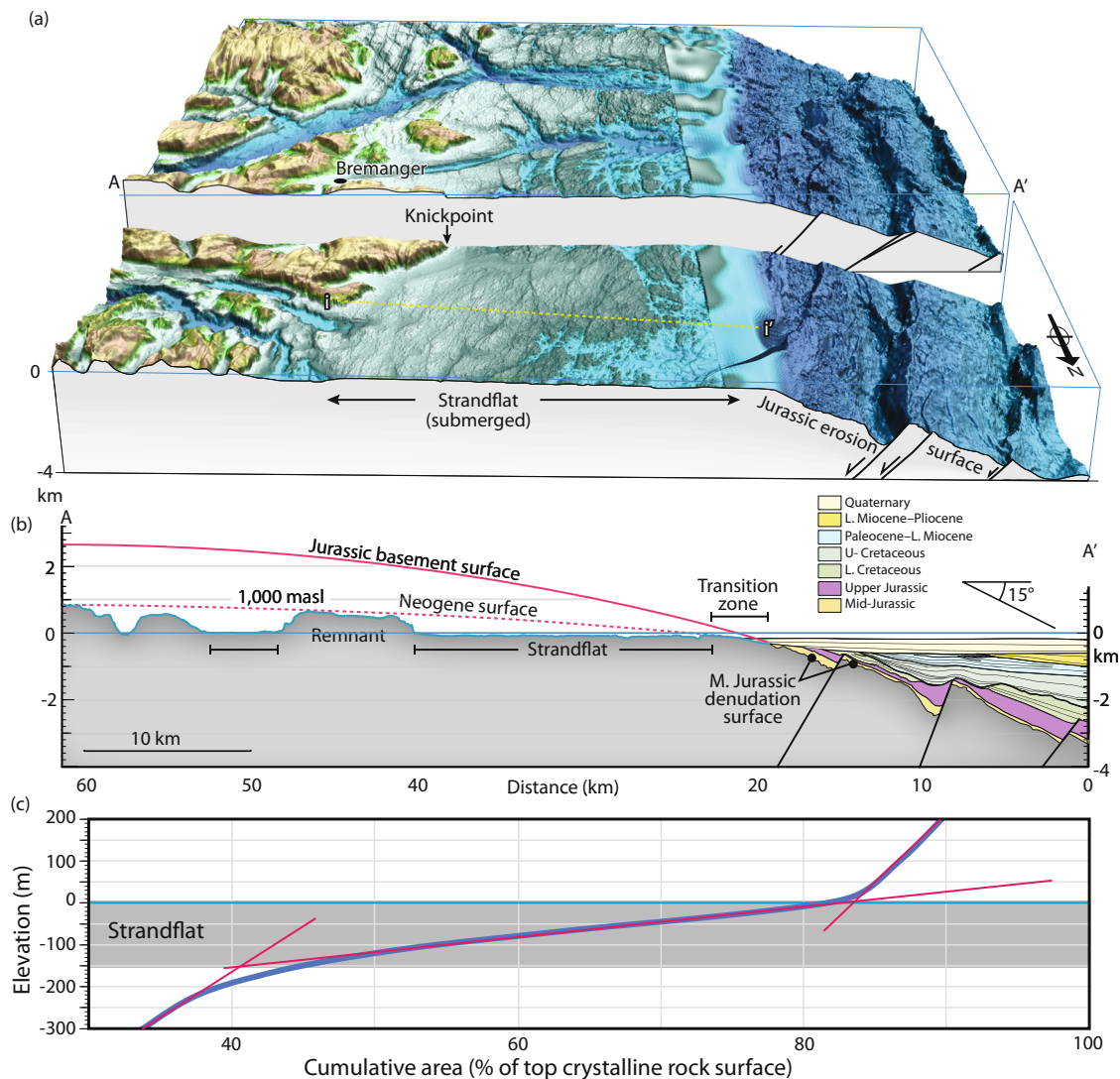


**Fig. 3** The strandflat in the northern part of the study area. **a** 3D model of the submerged strandflat in the Stad-Måløy Slope area, viewed from the north (2x vertical exaggeration, see Fig. 5 for location). Mesozoic sediments west of the strandflat have been removed. The subhorizontal strandflat is very well developed in this area, and the transition to the ca. 15° W-dipping bedrock surface to the west clearly defines its offshore limit (note that Mesozoic and younger sediments have been stripped off). Color scheme as for Fig. 2a. **b** shows the central section of **a** with its sedimentary offshore cover. **c** is the hypsometric curve for the area covered by **a**, allowing the main strandflat interval to be defined for the interval –150 m to near sea level.

rotation here relates to a major listric east-facing rift fault west of the study area. During this late Jurassic to early Cretaceous faulting, the Måløy Slope was flexed into a gigantic rollover structure (Supplementary Fig. S3). This structure abruptly terminates southwards at the rift transfer structure at the latitude of Sognefjorden. South of this fundamental transfer structure, the polarity of the rift system changes. Here, major west-dipping Permo-Triassic faults, such as the Øygarden fault, dominate the structural picture, with thick sequences of Triassic sediments in their hanging walls. Their limited Jurassic activity did not rotate Jurassic layers much (Fig. 5), and the near-shore Jurassic denudation surface east of the Øygarden fault dips gently to the west (Fig. 4). Also younger strata up to Neogene dip to the west, and most of this westerly dip can be attributed to coupled onshore uplift—offshore subsidence after the Mesozoic rifting. A regional angular unconformity separates the subhorizontal Quaternary deposits from underlying Neogene and older west-dipping sediments, and the last major phase of onshore uplift is therefore considered to be of Neogene age. The Neogene itself is characterized by extensive deltaic build-outs (Fig. 6)

linked to increased depositional rates that reflect onshore Neogene exhumation.

**The post-Mesozoic onshore denudation surface.** The onshore topography east of the strandflat is dominated by a system of elevated plateau elements (e.g., Fig. 7b) separated by fjords and valleys. Traditionally the plateaus are correlated into a topographic surface interpreted as an inherited pre-glacial landscape (the so-called paleic surface), reshaped by localized Pleistocene glacial, glaci-fluvial, and colluvial erosional processes. There is general consensus that the Pleistocene<sup>16</sup> fjords to a large extent represent pre-glacial fluvial drainage systems that were repeatedly exploited and many places severely deepened by glaciers. The largest fjord, the Sognefjord, was deepened to more than 1,000 m below current sea level, up to –1500 m in its central part<sup>16</sup>. The fjords shallow where they meet the strandflat, although many of them do show a westward continuation as relatively shallow channels through the strandflat (Figs. 2a and 3).

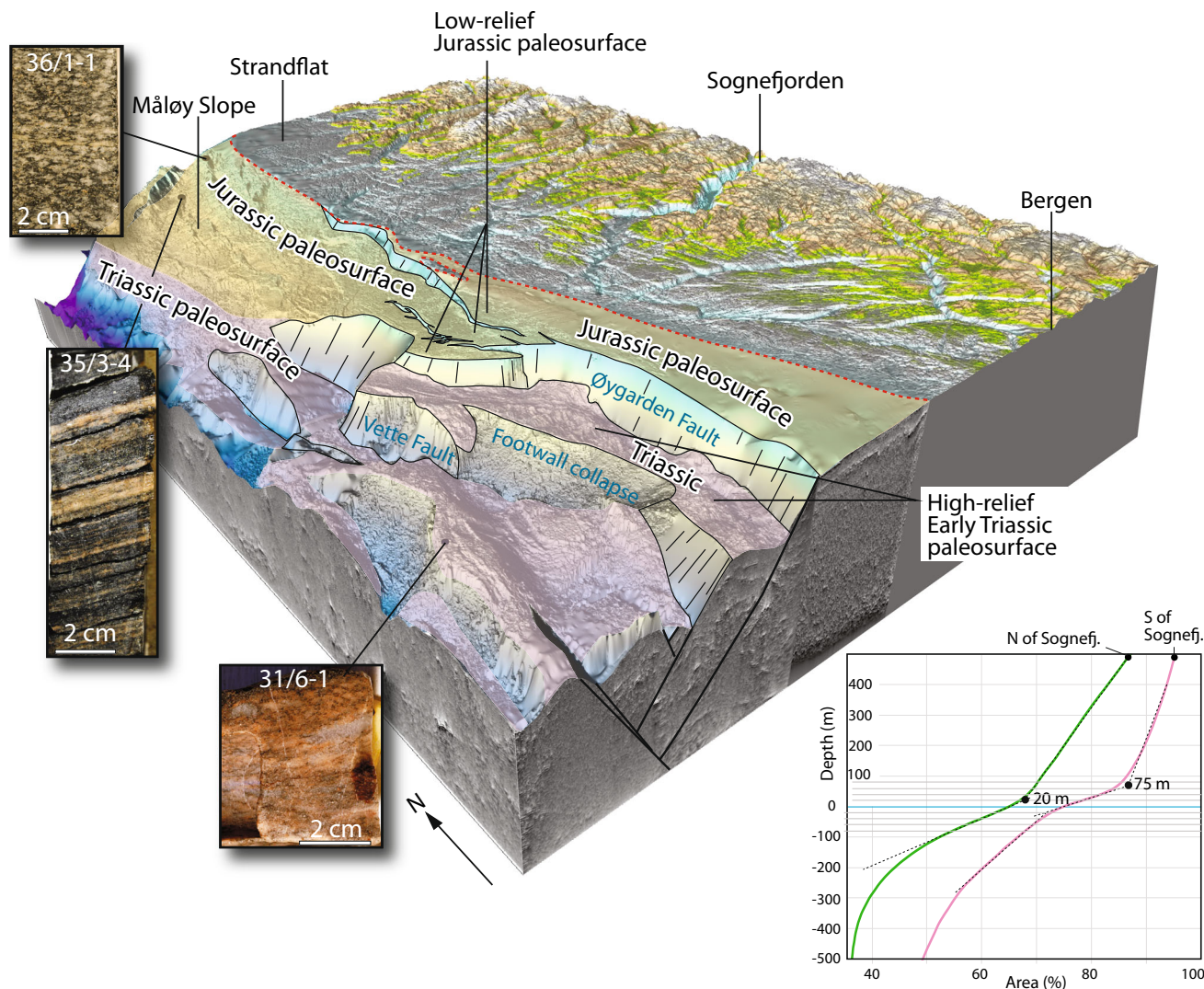


**Fig. 4 3D view of the top crystalline basement onshore-offshore from Bergen to Stad.** Offshore sediments have been removed to expose the basement. Three domains are recognizable: the glaciated onshore mountain-fjordscape, the near sea level strand flat, and the sloping and faulted paleo-topography of Jurassic and Triassic age. Figure prepared from onshore elevation data, bathymetric data and offshore seismic data. Graph shows hypsometric curves for the northern and southern parts of this area. The curves show a low-dip segment that relates to the strandflat, although the upper break in slope is better defined than their lower one. Both the upper and lower breaks in slope are lower for the northern part than for the southern part, reflecting the northward lowering of the strandflat.

The elevated plateaus between the fjords have been interpreted in different ways. Some regard them as a fragmented pre-glacial landscape surface that represents a mid-Jurassic peneplain capped at about 1 km altitude by a Miocene peneplain formed near sea level and elevated in the Pliocene<sup>17,18</sup>. Others argue that they represent remnants of a degraded base Cenozoic landscape surface<sup>19</sup> (Doré, 1992). This interpretation draws on the classical idealized interpretation of a low-level paleic surface (peneplain) that was uplifted from near-sea level to the current elevations of mountain peaks and plateaus<sup>20,21</sup>. If correct, it allows for this surface to be continued offshore as the base Cenozoic (Top Shetland Group) stratigraphic level.

There is, however, no strong evidence that the summits outline an isochronous surface of base Cenozoic or any other fixed age, and the fact that surfaces of different elevations coexist in the inland reflects the simplistic nature of this model. Others have therefore tried to classify plateaus of different elevations as being of different ages<sup>22</sup>. Obviously, such correlations are inherently difficult without independent dating. Surface dating without

stratigraphic constraints is difficult, and apatite fission track and (U-Th)/He thermochronometric data from the currently exposed peaks and mountainous plateaus east of the coastal region (the paleic surface) have been interpreted differently by different workers<sup>17,23</sup>. However, the simplest interpretation suggests that the rocks cooled slowly, and were probably some 1 to 3 km deep in the crust at the dawn of the Cenozoic<sup>24,25</sup>.

A completely different interpretation considers the high-elevation inland landforms as remnants of Caledonian mountains, modified during the Quaternary glaciations<sup>23,26,27</sup>. Nielsen et al.<sup>23</sup> suggest that it is unlikely for uplifted surfaces to be preserved over long geologic time spans, and that the flat summits of many Norwegian mountains (roughly connected in Fig. 6) therefore are unlikely to be erosional remnants of an uplifted Cretaceous or base Cenozoic paleic surface. In their model, glacial processes, particularly during the first part of the Pleistocene, are called for to explain not only the carving-out of fjords, but also extensive lowering of the mountain plateaus. Indeed, some middle way may be envisioned where the landscape

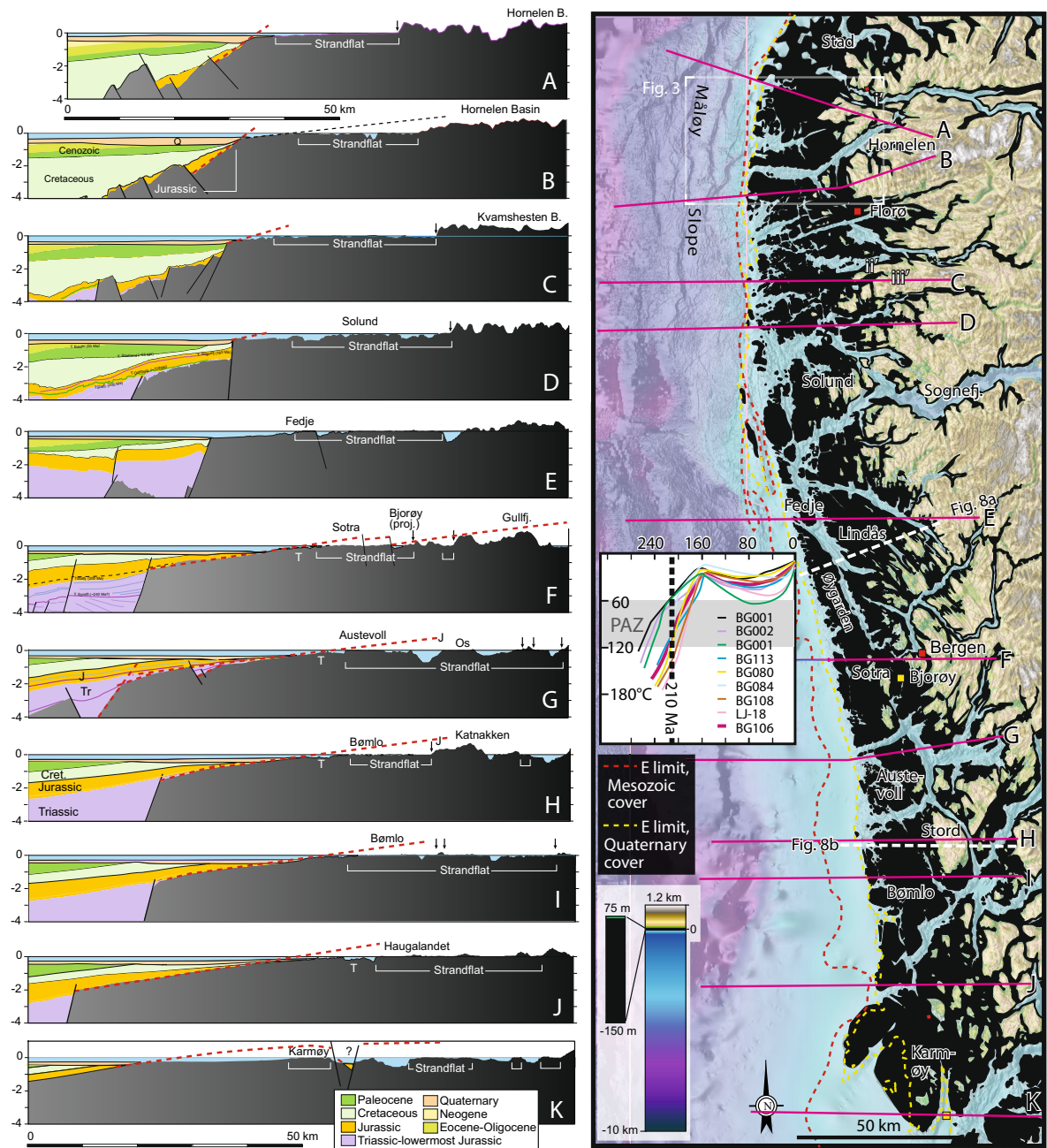


**Fig. 5 Profiles constructed across the on-offshore study area.** Profiles A-K (left panel) are based on topographic, bathymetric, and 3D seismic data. Dark gray is crystalline basement (including mildly metamorphosed Devonian sedimentary rocks). The sections are constructed approximately perpendicular to the trend of the strandflat. The main portion of the strandflat is annotated on the profiles, and the strandflat as well as near-sea level shoulders in the fjords are marked in black on the map (right panel). White dashed lines on the right panel are locations of profiles shown in Fig. 8. Inset graph in right panel shows time-temperature models (weighted mean paths) from apatite fission track and (U-Th)/He data from the strandflat near Bergen (mostly Øygarden-Sotra area), extracted from Ksienzyk et al. (2014). 210 Ma, the time of previously proposed weathering, is highlighted. PAZ; Partial Annealing Zone.

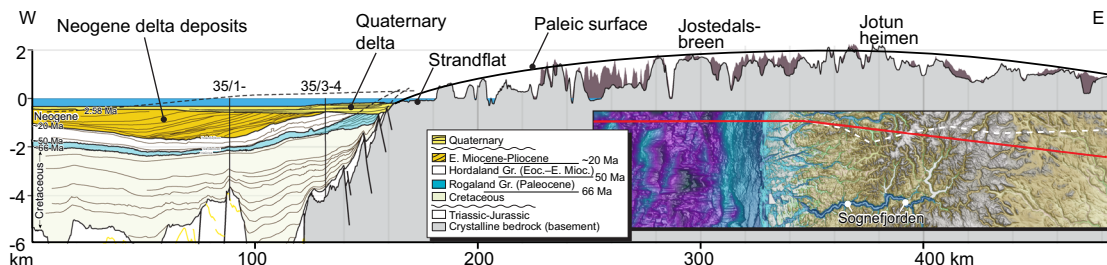


**Fig. 6 Regional section through South Norway-North Sea, with location map.** Offshore data show a km-thick wedge of Neogene delta deposits (20–2.58 Ma), downlapping onto Paleogene strata and unconformably overlain by Quaternary deposits. Inset map shows line location on a top crystalline bedrock map. Red line marks the main section, while white dashed line marks a secondary profile, projected onto the main section and shown in darker color.

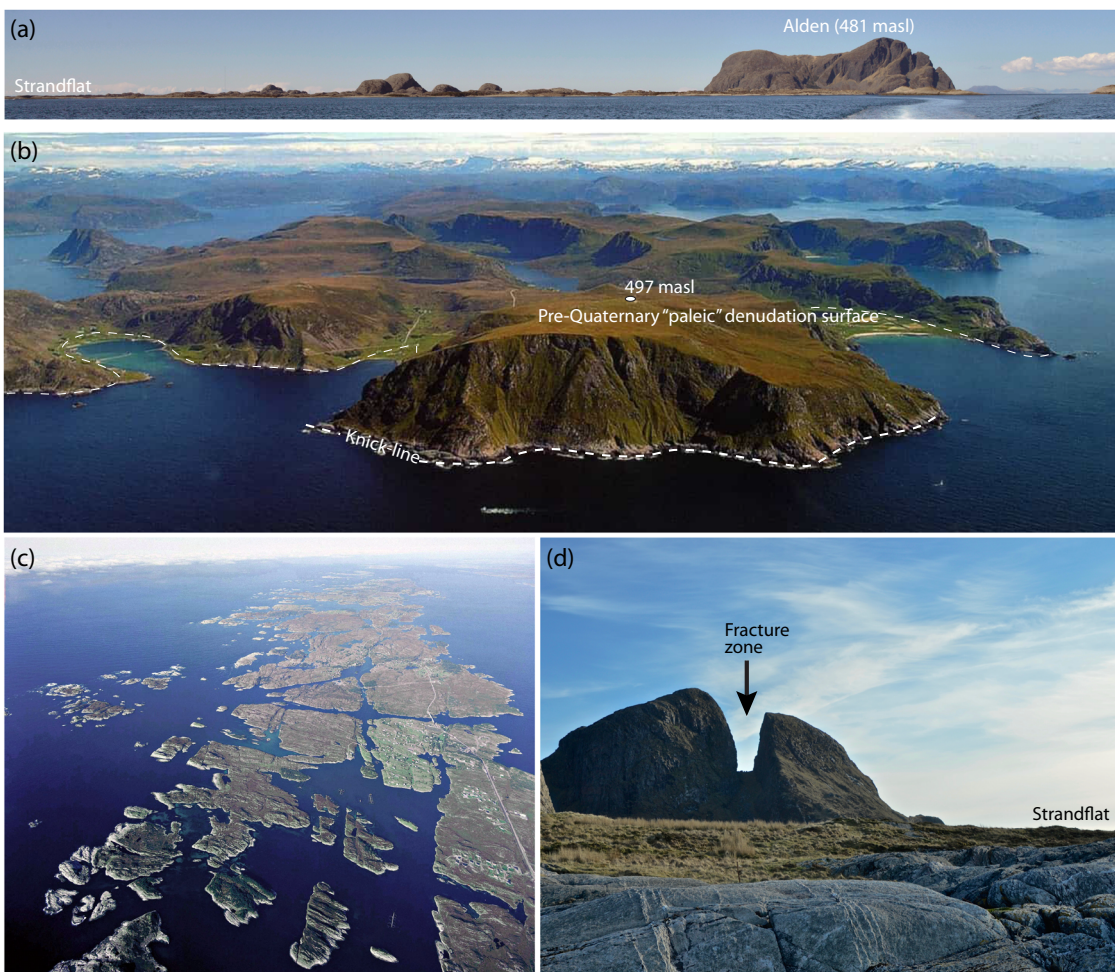


**Fig. 7 Photos of some characteristic strandflat features.** **a** Strandflat (mostly submerged) and remnant (monadnock) mountain Alden with further degenerated knobs to the left (west). **b** View to the E from the eastern limit against a higher and older plateau-like landscape in Stad. The landward limit of the subhorizontal strandflat is marked by a knick-line against a cliff-face that levels out to define an older “paleic” surface, in this area at around 400–500 m above sea level, with the highest peak of the peninsula at 645 m. Photo: J. Kråkenes. **c** The strandflat in Øygarden, teared up by fault and fracture zones. **d** Fracture zone, Kinn.

was never completely reduced to a near-sea level peneplane, but much lower than today’s landscape, elevated and eroded during Neogene uplift.

Regardless of its origin, it is evident that the strandflat was carved into a terrain defined by elevated surfaces and peaks whose enveloping surface dips towards the North Sea basin, and that this surface was subjected to glacial denudation that resulted in deep glacial valleys and fjords, most of which formed along pre-glacial drainage systems.

**The strandflat.** The eastern termination of the strandflat is many places well defined by an abrupt change in slope. This knickpoint is typically expressed by a steep cliff separating the subhorizontal strandflat from the several hundred meters higher hilly paleic surface (Fig. 7b). A similar marked change in slope defines the circumferential limit of isolated remnant hills or mountains (monadnocks, “nyker”) within the strandflat proper (Fig. 7a). Interestingly, the strandflat is also locally developed within the outer parts of the fjords, as narrow shoulders near sea level<sup>4</sup>.

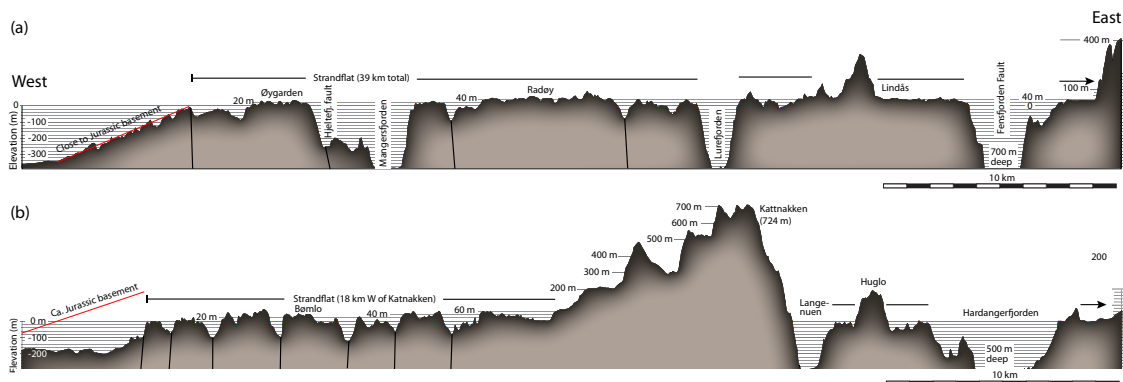


**Fig. 8 Two examples of detailed bathymetric profiles across the strandflat.** These highly (7x) vertically exaggerated sections reveal the finer-scale roughness and dip of the strandflat. In **a** the strandflat is broken up by fault-related fjords, but still well defined over a horizontal distance of almost 40 km, dipping on average  $0.3^\circ$  to the west. The transition zone is close to the Jurassic basement denudation surface. In **b** the strandflat is rougher, but still defining a close to horizontal orientation between 0–60 m in elevation. The summit of Kattnakken rises 700 m above the strandflat and may be relatively close to the late Jurassic erosion surface. See Fig. 5 for location.

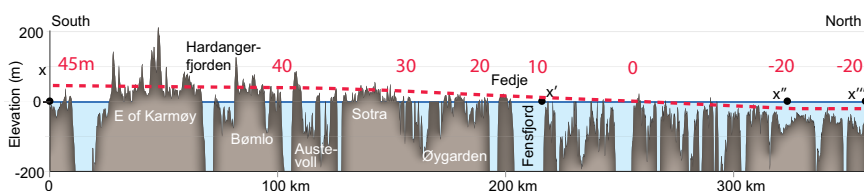


**Fig. 9 S-N profile along the coast.** The profile exhibits the northerly dip of the strandflat that closely matches the Younger Dryas isobase value (red dashed line), which varies from  $-35$  m in the south to  $-35$  m in the north. See Fig. 2a for location.

From these observations, the strandflat must be younger than the west-sloping paleic surface, and it must at least in part be developed after the Pleistocene fjords were eroded below sea level.

The western limit of the strandflat closely coincides with the occurrence of west-dipping Mesozoic sediments on basement, for instance in Profile A in Fig. 5. Most places, however, there is an up to 15 km wide transition zone between the clearly defined subhorizontal strandflat and in situ Mesozoic sediments (the area between the strandflat and the yellow dashed line in Figs. 2 and 5). The westward dip of this transition zone can be close to the Jurassic denudation surface (e.g., Profile *i* in Fig. 8) but is commonly denuded to a rougher and more gently dipping surface.

The 3D elevation model from the northern, mostly submerged part of the strandflat shown in Fig. 3 illustrates its main features well. New bathymetric data reveal this region as perhaps the best developed part of the strandflat in the study area in terms of width, continuity, smoothness and definition. Still, the strandflat is also here broken up by deeper channels and fault-related lineaments, and it is decorated by several monadnocks (Fig. 6a). The eastern boundary shows the characteristic steep cliff against the paleic surface. The data shows how this paleic surface is lower and younger than the extrapolated Jurassic topographic level (Fig. 3b and red dashed lines in Fig. 5), and higher and older than the strandflat.

The strandflat is less rough than the offshore unconformity and the inland topography, but has developed numerous irregularities at the vertical scale of  $\pm 10$  to  $\pm 20$  m (Fig. 8). In spite of these smaller irregularities, many of which define slightly different horizontal levels within the strandflat domain, the subhorizontal orientation of the strandflat is easily defined. A very gentle

westerly slope can be identified, amounting to just a few tens of meters of elevation difference across the strandflat in many cases. As an example, section a in Fig. 8 from the strandflat between Bergen and Sognefjorden shows how it is separated into  $\sim 10$  km wide sections by three fault-controlled fjords (Fensfjorden, Lurefjorden, and Hjeltefjorden). The strandflat is defined at roughly 30–40 m above the current sea level from the east across Lindås and Radøy, dropping to 10–20 m in the western part. A larger variation (0–60 m) is seen from Profile 8b, with the highest levels in the central part. In most of the study area, the average slope of the strandflat is close to that predicted by glacioisostatic uplift since the Younger Dryas ( $1.3 \text{ m km}^{-1}$  28). In Fig. 8a, the strandflat appears more horizontal than expected from this postglacial uplift (45 m from the eastern knickpoint through Øygarden, while the observed lowering is around 25–30 m). These variations probably reflect that different parts of the strandflat were formed at periods of different relative sea level.

There is also a general northward lowering of the strandflat parallel to the coast, from the south where most of the strandflat is situated above the present sea level to the north where effectively the entire strandflat is submerged (Fig. 9). This coast-parallel variation is fully explained by differences in glacio-isostatic uplift since the Younger Dryas around 11,700 years ago. The post-glacial isobase map for the study area<sup>4</sup> shows a variation from approximately 35 m east of Karmøy to  $-35$  m in the north that closely matches the variation in strandflat altitude shown in Fig. 9.

Another important feature of the strandflat is the lack of strong Holocene erosion around sea level. In other words, there is no sign of strandflat development since the end of the last glaciation.



This is documented by the preservation of fresh glacial striae on the strandflat, also south of Sognefjorden<sup>28</sup> where the strandflat has been uplifted relative to sea-level since the Younger Dryas. Any further evolution of the strandflat would be exposed in this area, while it might have been submerged to the north. Hence, the strandflat must have formed by processes that were active at different and probably colder climatic conditions than the current ones.

### Origin of the strandflat

The horizontality of the strandflat and the way it sharply cuts through the rotated offshore Jurassic denudation surface and overlying pre-Quaternary strata as well as the younger paleic surface onshore is compelling evidence of a Quaternary age. The preservation of abundant glacial striae on the strandflat gives an upper age constraint of Younger Dryas, the last glacial advance to the coastal areas in the region. Although this is compelling evidence that the strandflat must be Pleistocene in age, alternative models are discussed below.

**Triassic weathering and inheritance.** The alternative model where the strandflat is an “inherited Mesozoic landscape”, or “rejuvenated geomorphic relic from Mesozoic times”, formed by stripping off Mesozoic strata<sup>10</sup>, is incompatible with the new data presented in this work. Any inherited Mesozoic landscape would be west dipping, at as much as 15° north of Sognefjorden. In the south, particularly south of Bømlo, the dip is lower, but still clearly different from the subhorizontal strandflat. Also, the deep late Triassic weathering proposed for the strandflat area is questionable, since evidence for such weathering is not found in cores from the offshore rift margin (e.g., wells 36/1-1, 31/6-1, 35/3-4; 18/11-1, 17/3-1). This is corroborated by the high-amplitude seismic reflection signal from the Jurassic basement surface west of the strandflat. Basement weathering has been identified some 200 km SW of the strandflat, in the Utsira basement high. Here, some 20 m of Mesozoic regolith has been documented from a few wells (notably 16/1-15 and 16/3-4), while the majority of basement wells in the area entered poorly weathered or unweathered basement. Within the strandflat itself, Jurassic sediments occurring in the Bjørøy fault zone are in contact with basement gneiss with up to a couple of meters of alteration. However, being located in a fault zone, this relatively modest alteration may be ascribed to fault zone alteration and not necessarily Jurassic surface weathering<sup>14</sup>. Furthermore, the coastal area underwent extensive erosion throughout the Triassic and into the Jurassic, as reflected by thick Triassic deposits immediately to the west (Fig. 5) and thermochronologic data<sup>29</sup>. Considering these observations, it seems highly unlikely to infer hundreds of meters of wide-spread Triassic weathering in the strandflat area. On the other hand, it is likely that some patches of inherited Mesozoic landscape may by chance be preserved in the strandflat region, notably in the Bjørøy area, where the Jurassic landscape is downfaulted to the east, and from Karmøy and southwards where the strandflat gradually vanishes. However, such possible relics of Jurassic landscape would not be part of the subhorizontal strandflat, which Fredin et al. (2017)<sup>30</sup> imprecisely claim was expressed by Fossen et al. (2017)<sup>13</sup>. Instead, the strandflat indiscriminately cuts horizontally through any earlier landform like a buzz saw.

A completely independent set of data that can be used to test the model of Mesozoic landscape inheritance is low-temperature thermochronologic data. Although such data need to be interpreted with care, fission track and (U–Th)/He-data from the strandflat and the adjacent inland region shows a consistent pattern of cooling (2–3 °C My<sup>-1</sup>) until the late Jurassic. Modeled cooling paths for nine samples from the strandflat north, west and east of Bergen are shown in the inset graph in Fig. 5. The curves, constrained by

near-surface (0–30 °C) conditions in the late Jurassic, consistently indicate temperatures of 60–150 °C, or 2–5 km of burial in the late Triassic (210 Ma)—the previously proposed time of weathering. Indeed, weathering to 2–5 km depth is unrealistic under any physio-climatic conditions. Weathering-like hydrothermal alteration with illite growth within fault zones in Western Norway, however, is well documented to give Mesozoic ages<sup>11</sup>, and the Bømlo illite ages fit this data very well.

**Strandflat-forming processes.** Since the strandflat has not developed any further after the last glaciation, it must involve processes favored during colder Quaternary climate, but in periods with no or limited coastal ice coverage. Such cold-climate processes are mainly local glacial erosion, frost-shattering, and sea-ice abrasion. Wave abrasion can also relate to cold climate, being more effective when operating with sea-ice. However, it has been pointed out that wave abrasion should affect oceanward sides much more effectively than sheltered land-facing cliffs, while no such asymmetry is found neither in Western Norway nor in other similar strandflat regions<sup>31</sup>. Hence, wave processes can be considered secondary.

Local glacial erosion can occur where cirque glaciers cut back into mountain slopes—a process proposed based on observations from Antarctica<sup>32</sup> (Holtedahl, 1929). In cold climate, such glaciers could occur along the coast all the way to sea level, producing strandflat elements that could be further developed by other erosional processes. Examples of cirque glaciers cutting down to sea level is found in the study area, particularly along Fensfjorden (Supplementary Fig. S4). However, slow erosion rates also make cirque erosion a secondary process<sup>5</sup>. Glacial erosion at times of continuous ice coverage, i.e., glacial maxima, can be regarded as small in the coastal area, because the strandflat was then mostly below sea level due to glacio-isostatic depression of the crust. However, glacial shoveling during the repeated glacial advances must have removed debris from the strandflat, as would waves together with sea-ice.

Both Nansen<sup>1,2</sup> and Larsen and Holtedahl<sup>5</sup> favored frost-shattering along sea cliffs together with sea-ice erosion as the main strandflat forming processes. Late Weichselian rock platforms are common along the fjords of northern Norway and described as formed mainly by frost weathering just outside the Younger Dryas glacier terminus<sup>33,34</sup>. Periglacial lacustrine frost weathering of Holocene age is also recorded at higher altitudes with colder climate than the coastal area and with freshwater with its higher freezing temperature as an agent. Rapid rock platform formation by was reported by Matthews et al.<sup>35</sup> from a lake in Jotunheimen in southern Norway. This cryoplanated rock platform is up to 5.3 meters wide and formed along an ice-dammed lake that existed for only 200 years (dated to AD 1650–1850). Erosion rates ranging from 1.4–7.1 cm y<sup>-1</sup> were estimated by means of lichenometry, <sup>14</sup>C dating, Schmidt hammer values, and historical data. Aarseth and Fossen<sup>36,37</sup> interpreted a 20 m Holocene (<6000 years) platform along a lake northeast of Bergen to have formed as a result of high precipitation and frequent freeze-thaw cycles during winter. The cryoplanated platform was found to be much better developed in strongly foliated rocks (schists) than in more massive granitic gneisses and serpentinite. Some larger lower-altitude lake platforms in the Bergen area were also interpreted to have formed by cryoplanation (frost weathering), but during Weichselian (late Quaternary) interstadials. These observations suggest that cryoplanated surfaces of tens of meters can form over short (1000-year or even 100-year scale) time periods. They strengthen the impression of frost-shattering as an important, perhaps the most important, strandflat-forming mechanism.

**The important role of faults and fractures.** The strandflat platform is fragmented by faults and fracture zones that stand out

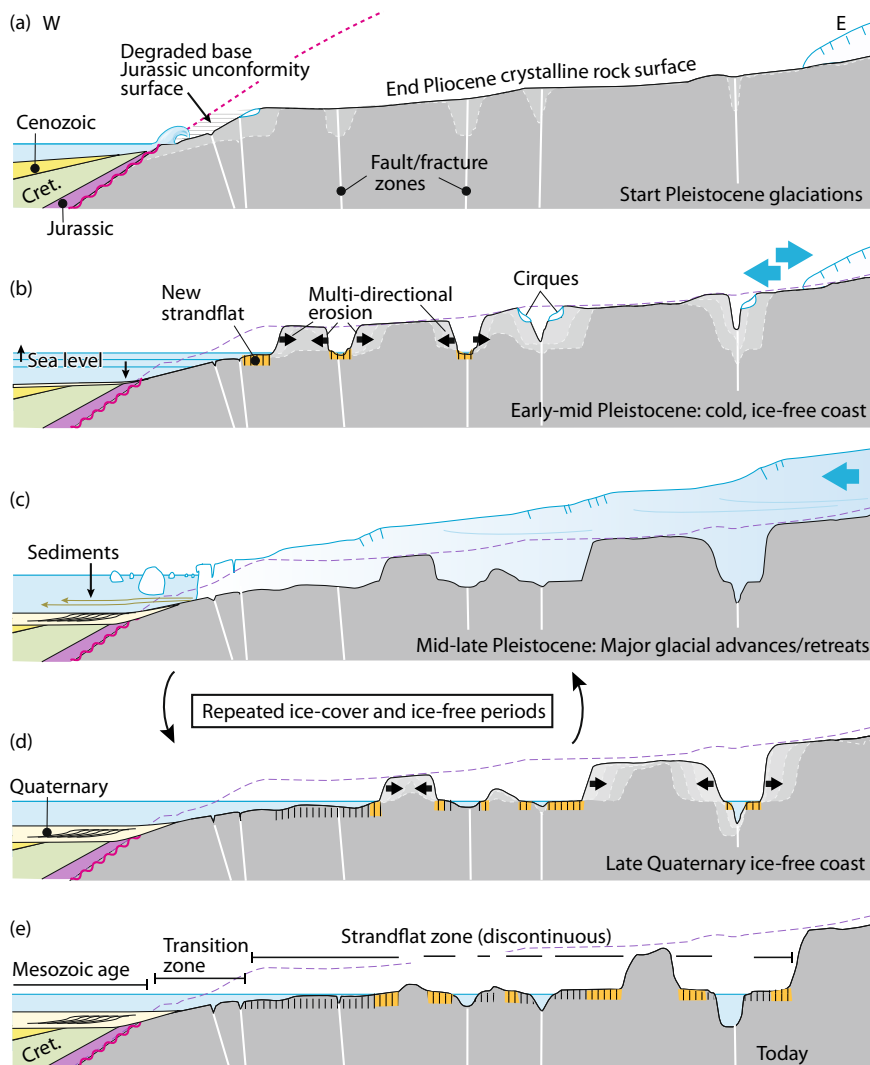


**Fig. 10 Schematic evolutionary model for the strandflat from the start of the Pleistocene until today.** **a** The situation at the start of the Pleistocene, with a gently W-dipping elevated onshore topographic surface. This paleic surface is younger than the steeper base Jurassic unconformity to the west. **b** Strandflat-forming cold-climate erosion during ice-free periods. The area is repeatedly covered by glaciers (**c**) that remove erosion products from the strandflat, before returning to ice-free conditions (**d**). No further development of the strandflat occurred in the Holocene, so **e** represents both the current and the end Pleistocene situation. Orange fields mark the most recent parts of the strandflat at any given time. Throughout, erosion was guided by fault and fracture zones, simultaneously acting in different directions at different locations. Overall, however, the inner (eastern) part of the strandflat is the youngest part. Note that the strandflat is generally wider than shown here.

as topographically negative scars (Fig. 7d), sounds (Fig. 7c), and narrow valley and even fjords (Fensfjorden, Hjeltefjorden) of straight or gently curved geometry. Interestingly, their frequency as measured perpendicular to the coast has been shown to increase by a factor of 2–4 from the inland and into the strandflat area, likely related to its proximity to the main North Sea rift (Fossen et al., 2021). Within the strandflat elements, smaller faults and fractures down to the meter scale are numerous and with more diverse orientations.

Erosion processes such as frost-shattering rely heavily on fractures<sup>38</sup>, and the breaking off of chunks of rock layers along fractures can be observed all along the coast. Mechanical and chemical alteration of larger zones, with the formation of incohesive fault gouge and dense fracture networks is also widespread. Such weak zones localize weathering and erosion that deepen and widen the zone, which allows for simultaneous erosion at multiple locations and in multiple directions, greatly speeding up the overall rate of strandflat formation. On top of this comes variable foliation development in the bedrock, which

helps explain the somewhat narrower strandflat in massive granitic rocks than in schists (Supplementary Fig. S5).

**Could the strandflat be formed during the Pleistocene?** While it is clear that the strandflat is a Pleistocene geomorphic feature formed by cold-climate erosional processes, its formation must have been discontinuous, depending on the cyclic climatic variations in this period. The optimal thermal conditions would be when temperatures were colder than today, but without much or any ice-cover, especially in a periglacial environment. This occurred at the beginning and, for a shorter period also at the end each glacial period. Almost the entire Early (2.6–0.8 My) Pleistocene was colder than today, but with cyclic variations. It is characterized by 41 cold stages, of which 14 show evidence of major glaciation<sup>39</sup>. Hence the coastal area was cold and ice-free for most of this period. With a change from 41 ky to 100 ky cycles, the last ~0.9 My were dominated by 5–6 extensive glacial periods separated by much shorter interstadials. Only for a few tens of thousands of years during the

last million years did the temperature reach Holocene levels, but the coast was repeatedly covered by ice, so the time of strandflat erosion was probably 50% or less. Although somewhat speculative, it seems reasonable to assume that strandflat erosion was effective for close to 50% of the entire Pleistocene period, i.e., for around 1 My. If we use the cryoplanation erosion rate of  $1.4\text{--}7.1\text{ cm y}^{-1}$  from Matthews et al.<sup>35</sup>, that could generate a unidirectional strandflat width of 14–71 km, which covers the final width of the strandflat (20–40 km in the study area). Similar cliff retreat rates in crystalline rocks from Norway and Scotland were reported by other authors<sup>34,40–42</sup>. Considering that the strandflat widened from several locations simultaneously due to fault-controlled valleys and sounds, and adding the effect of secondary erosion processes, the erosion rate or time period of active strandflat formation could be greatly reduced. I, therefore, conclude that there is enough time for the strandflat to develop entirely within the Pleistocene period, and that conditions were optimal in terms of long cumulative cold periods with an ice-free coast to produce the extensive Norwegian strandflat, which is both wider and longer than those seen elsewhere at both high and low latitudes, notably in Scotland<sup>43</sup>, Antarctica<sup>31</sup>, Labrador and Alaska<sup>43</sup>.

Our study demonstrates that shore-platform formation in crystalline rocks in high-latitude regions is efficient in cold climate, and that the subarctic strandflat along the west coast of Norway only developed during Pleistocene ice-free periods under colder conditions than the Holocene (Fig. 10). While faults and fractures have passed unnoticed in earlier discussion of the strandflat, I stress that the high frequency of such structures along the coast promoted strandflat-forming processes and contributed to the impressive width of the strandflat. The previously proposed model of frost-shattering as the primary, but not only, erosional process is supported, while the alternative model where the strandflat is thought to be a re-exposed Mesozoic weathering surface is refuted.

## Methods

**Seismic data interpretation.** Interpretation of depth-converted commercial offshore seismic broadband data (NVG N-S survey) provided by CGG (egg.com) was performed by means of Petrel software at top crystalline basement, top Staftjord Fm., top Oseberg Fm., top Brent Grp., base Cretaceous, several Paleogene to Neogene horizons and base Quaternary levels, of which the top basement interpretation was primarily used in this project. Available 2D regional lines were depth converted and used in areas outside of the coverage of the broadband data and an interpolated version of the interpretation was merged with the 3D seismic top basement interpretation.

**Integrated digital elevation model.** National elevation data (10 m resolution) and bathymetric data (50 m resolution) from the Norwegian Mapping Authority (kartverket.no) were merged using Petrel and QGIS. In this process, the model was cut off where thick Quaternary sediments cover older sediments and rocks. This boundary was picked from the morphology of the seabed. In areas where 50 m cell size bathymetric data are missing, an interpolated bathymetric dataset was used.

The resulting elevation model was then merged with the seismic top basement interpretation to a seamless elevation/depth model that was used for further analysis, including dip and roughness analyses performed in QGIS.

## Data availability

Elevation and bathymetric data used are public data, separately downloadable from [www.kartverket.no](http://www.kartverket.no) or [www.geonorge.no/](http://www.geonorge.no/). Offshore seismic data are property of CGG (CGG.com), and interpretations derived from those data are not public, except for the figures themselves as presented in this article.

Received: 10 November 2022; Accepted: 21 February 2023;

Published online: 07 March 2023

## References

- Nansen, F. The bathymetrical features of the North polar seas. In Nansen, F. (ed.): The Norwegian North Polar Expedition 1893–1896. *Scientific results IV*. J. Dybwad, Christiania, 1–232 (1904).
- Nansen, F. The strandflat and isostasy. *Skr. Vid. Selsk. Krist. Mat.-Naturvid. Kl. 2*, 1–313 (1922).
- Holtedahl, O. Den norske strandflate. Med særlig henblikk på dens utvikling i kystområdene på Møre. *Norsk Geogr. Tidsskr.* **16**, 285–305 (1959).
- Holtedahl, H. The Norwegian strandflat—a geomorphological puzzle. *Norsk Geol. Tidsskr.* **78**, 47–66 (1998).
- Larsen, E. & Holtedahl, H. The Norwegian strandflat: a reconsideration of its age and origin. *Norsk Geol. Tidsskr.* **65**, 247–254 (1985).
- Ahlmann, H. W. Geomorphological studies in Norway. *Geogr. Ann.* **1**, 193–252 (1919).
- Evers, W. The Problem of Coastal Genesis, with Special Reference to the “Strandflat,” the “Banks,” or “Grounds,” and “Deep Channels” of the Norwegian and Greenland Coasts. *J. Geol.* **70**, 621–630 (1962).
- Askland, B. Strandflaten på Sveriges Västkust. Referat fra foredrag holdt på møte 1 november 1928. *GFF* **50**, 801–810 (1928).
- Olesen, O. et al. Deep weathering, neotectonics and strandflat formation in Nordland, northern Norway. *Norw. J. Geol.* **93**, 189–213 (2013).
- Fredin, O. et al. The inheritance of a Mesozoic landscape in western Scandinavia. *Nat. Commun.* **8**, 14879 (2017).
- Ksienzyk, A. K. et al. Post-Caledonian brittle deformation in the Bergen area, West Norway: results from K-Ar illite fault gouge dating. *Norw. J. Geol.* **96**, 275–299 (2016).
- Fossen, H., Ksienzyk, A. K., Rotevatn, A., Bauck, M. S. & Wemmer, K. From widespread faulting to localised rifting: Evidence from K-Ar fault gouge dates from the Norwegian North Sea rift shoulder. *Basin Res.* **33**, 1934–1953 (2021).
- Fossen, H., Ksienzyk, A. K. & Jacobs, J. Correspondence: Challenges with dating weathering products to unravel ancient landscapes. *Nat. Commun.* **8**, 1502 (2017).
- Fossen, H., Mangerud, G., Hesthammer, J., Bugge, T. & Gabrielsen, R. The Bjorøy Formation: a newly discovered occurrence of Jurassic sediments in the Bergen Arc System. *Norsk Geol. Tidsskr.* **77**, 269–287 (1997).
- Bauck, M.S., Faleide, J.I. & Fossen, H. Late Jurassic to Late Cretaceous canyons on the Måløy Slope: Source to sink fingerprints on the northernmost North Sea rift margin, Norway. *Norw. J. Geol.* **101** <https://doi.org/10.17850/njg101-3-1> (2021).
- Nesje, A. & Whillans, I. M. Erosion of Sognefjord, western Norway. *Geomorph* **9**, 33–45 (1994).
- Japsen, P., Green, P. F., Chalmers, J. A. & Bonow, J. M. Mountains of southernmost Norway: uplifted Miocene peneplains and re-exposed Mesozoic surfaces. *J. Geol. Soc.* **175**, 721–741 (2018).
- Riis, F. Quantification of Cenozoic vertical movements of Scandinavia by correlation of morphological surfaces with offshore data. *Glob. Planet. Change* **12**, 331–357 (1996).
- Doré, A. G. The base Tertiary surface of southern Norway and the northern North Sea. *Norsk Geol. Tidsskr.* **72**, 259–265 (1992).
- Reusch, H. Strandflaten, et nyt træk i Norges geografi. *Nor. Geol. Unders. B.* **14**, 1–14 (1894).
- Gjessing, J. Norway’s paleic surface. *Norsk Geogr. Tidsskr.* **21**, 69–132 (1967).
- Lidmar-Bergström, K., Näslund, J.-O., Ebert, K., Neubeck, T. & Bonow, J. M. Cenozoic landscape development on the passive margin of northern Scandinavia. *Norw. J. Geol.* **87**, 181–196 (2007).
- Nielsen, S. B. et al. The evolution of western Scandinavian topography: A review of Neogene uplift versus the ICE (isostasy–climate–erosion) hypothesis. *J. Geodyn.* **47**, 72–95 (2009).
- Hendriks, B. H. W. et al. A fission track data compilation for Fennoscandia. *Norw. J. Geol.* **87**, 143–155 (2007).
- Johannessen, K. C., Kohlmann, F., Ksienzyk, A. K., Dunkl, I. & Jacobs, J. Tectonic evolution of the SW Norwegian passive margin based on low-temperature thermochronology from the innermost Hardangerfjord area. *Norw. J. Geol.* **93**, 243–260 (2013).
- Steer, P., Huismans, R. S., Valla, P. G., Gac, S. & Herman, F. Bimodal Plio–Quaternary glacial erosion of fjords and low-relief surfaces in Scandinavia. *Nat. Geosc.* **5**, 635–639 (2012).
- Pedersen, V. K. et al. Widespread glacial erosion on the Scandinavian passive margin. *Geology* **49**, 1004–1008 (2021).
- Mangerud, J., Hughes, A. L. C., Sæle, T. H. & Svendsen, J. I. Ice-flow patterns and precise timing of ice sheet retreat across a dissected fjord landscape in western Norway. *Quat. Sci. Rev.* **214**, 139–163 (2019).
- Ksienzyk, A. K., Dunkl, I., Jacobs, J., Fossen, H. & Kohlmann, F. From orogen to passive margin: constraints from fission track and (U-Th)/He analyses on Mesozoic uplift and fault reactivation in SW Norway. *Geol. Soc. Lond. Spec. Publ.* **390**, 679–720 (2014).
- Fredin, O. et al. Reply to ‘Challenges with dating weathering products to unravel ancient landscapes’ *Nat. Commun.* **8**, <https://doi.org/10.1038/s41467-017-01468-6> (2017).
- Hansom, J. D. Shore-platform development in the South Shetland Islands, Antarctica. *Marine Geol.* **53**, 211–229 (1983).
- Holtedahl, O. On the geology and physiography of some Antarctic and sub-Antarctic islands. Scientific results of the Norwegian Antarctic Expedition 1927–1928. *Det Norske Videnskaps-Akademi, Oslo* **3**, 172p (1929).

33. Marthinussen, M. Coast and fjord area of Finnmark with remarks on some other districts. *Nor. Geol. Unders. B.* **208**, 416–429 (1960).
34. Rasmussen, A. The deglaciation of the Coastal area NW of Svartisen, northern Norway. *Nor. Geol. Unders. B.* **369**, 1–31 (1981).
35. Matthews, J. A., Dawson, A. G. & Shakesby, R. A. Lake shoreline development, frost weathering and rock platform erosion in an alpine periglacial environment, Jotunheimen, southern Norway. *Boreas* **15**, 33–50 (1986).
36. Aarseth, I. & Fossen, H. A Holocene lacustrine rock platform around Storavatnet, Osterøy, western Norway. *Holocene* **14**, 589–596 (2004).
37. Aarseth, I. & Fossen, H. Late Quaternary, cryoplanation of rock surfaces in lacustrine environments in the Bergen area, Norway. *Norw. J. Geol.* **84**, 1225–1137 (2004).
38. Matthews, J. A. et al. Age and development of active cryoplanation terraces in the alpine permafrost zone at Svartkampan, Jotunheimen, southern Norway. *Quat. Res.* **92**, 641–664 (2019).
39. Ehlers, J., Gibbard, P.L. & Hughes, P.D. Quaternary glaciations and chronology. In: *Past Glacial Environments*, <https://doi.org/10.1016/B978-0-08-100524-8.00003-8> (2018).
40. Jahn, A. Quantitative analysis of some periglacial processes in Spitsbergen. Uniwerstet Wrocklawski im Boleslawa Bieruta, *Zeszyty Nauk. Nauki Przyrodnicze II*, Warsaw (1961).
41. Dawson, A. G. 1980. Shore erosion by frost: an example from the Scottish Lateglacial. In *Studies in the Lateglacial of NW Europe* (eds J. J. Lowe, J. M. Gray & J. E. Robinson), pp. 45–53. Oxford University Press.
42. Dawson, A. G., Matthews, J. A. & Shakesby, R. A. Rock platform erosion on periglacial shores: a modern analogue for Pleistocene rock platforms in Britain. In *Pleistocene Periglacial Processes and Modern Analogues* (ed. J. Boardman), pp. 173–182. Cambridge University Press (1987).
43. Holtedahl, H. Some remarks on geomorphology of continental shelves off Norway, Labrador, and Southeast Alaska. *J. Geol.* **66**, 461–471 (1958).

### Acknowledgements

We thank Tim Redfield, Per-Terje Osmundsen, and an anonymous reviewer for useful reviews, and Atle Nesje for comments. Seismic company CGG is thanked for allowing access to their broadband 3D seismic data and publication of interpretations based on these data.

### Author contributions

All work by the author.

### Funding

Open access funding provided by University of Bergen.

### Competing interests

The author declares no competing interests.

### Additional information

**Supplementary information** The online version contains supplementary material available at <https://doi.org/10.1038/s43247-023-00724-6>.

**Correspondence** and requests for materials should be addressed to Haakon Fossen.

**Peer review information** *Communications Earth & Environment* thanks Per Terje Osmundsen, Tim Redfield, and the other, anonymous, reviewer(s) for their contribution to the peer review of this work. Primary Handling Editors: Maria Laura Balestrieri and Joe Aslin.

**Reprints and permission information** is available at <http://www.nature.com/reprints>

**Publisher's note** Springer Nature remains neutral with regard to jurisdictional claims in published maps and institutional affiliations.



**Open Access** This article is licensed under a Creative Commons Attribution 4.0 International License, which permits use, sharing, adaptation, distribution and reproduction in any medium or format, as long as you give appropriate credit to the original author(s) and the source, provide a link to the Creative Commons license, and indicate if changes were made. The images or other third party material in this article are included in the article's Creative Commons license, unless indicated otherwise in a credit line to the material. If material is not included in the article's Creative Commons license and your intended use is not permitted by statutory regulation or exceeds the permitted use, you will need to obtain permission directly from the copyright holder. To view a copy of this license, visit <http://creativecommons.org/licenses/by/4.0/>.

© The Author(s) 2023